

OMAE2017-62103

**ON THE FEASIBILITY OF USING UNDERWATER ACOUSTIC DATA TRANSMISSION FOR
SUBSEA EQUIPMENT MONITORING**

Bessie A. Ribeiro

Subsea Technology Laboratory - COPPE
Federal University of Rio de Janeiro, Brazil
Email: bessie@lts.coppe.ufrj.br

Viviane R. Barroso

Sonar Technology Laboratory - COPPE
Federal University of Rio de Janeiro, Brazil
Email: vivianerodrigues@oceanica.ufrj.br

Viviane F. da Silva

Subsea Technology Laboratory - COPPE
Federal University of Rio de Janeiro, Brazil
Email: vivianeferreira1002@gmail.com

Fabio C. Xavier

Institute of Sea Studies Admiral Paulo Moreira
IEAPM - Brazil Navy (MB)
Email: fabiofcx@gmail.com

Theodoro A. Netto

Subsea Technology Laboratory - COPPE
Federal University of Rio de Janeiro, Brazil
Email: tanetto@lts.coppe.ufrj.br

ABSTRACT

The present work uses the BELLHOP ray tracing model to simulate an acoustic propagation channel in a deep water environment in order to analyze its viability to provide data transmission for monitoring submarine equipment. The simulated scenario is located in the Campos Basin, Rio de Janeiro, on the Brazilian coast, responsible for more than 80% of Brazilian oil and gas production. Temperature and salinity data from five stations were used to calculate the sound speed profiles required to the transmission loss simulations of the acoustic propagation channel. In order to estimate the signal detection capacity according to the medium characteristics, a characterization of the parameters that influence the physical propagation channel was performed. The parameters of three modem models with different operation frequencies were selected and analyzed in order to obtain the Signal to Noise Ratio (SNR) of the transmission signal.

1. INTRODUCTION

The underwater data transmission for remote monitoring of subsea systems has been studied in several research areas [1-3]. Among potential applications are the transmission of metocean and imaging data, oil spill detection, monitoring of marine bio-systems, identification of military targets, vehicle control and so on. In case of subsea production systems, the main advantage of constant monitoring of the equipment include the ability to evaluate underwater facilities in deep water scenarios for early detection of eventual non-conformities or failures. The development of systems that enable data acquisition and access in a fast and versatile way is taken into account for immediate decision making [4].

Underwater wireless communication are made possible by optical, electromagnetic and acoustic wave propagation [5]. Despite providing high transmission rates, optical signal dispersion in seawater, due physical parameters such as turbidity and particles, limits the use of this technology over

short distances by ensuring high transmission rates in situations where the transceivers are in line of sight [6]. On the same way, in subsea environments the electromagnetic waves presents limited range due the high conductivity of the seawater, leading to signal attenuation. As a consequence, electromagnetic waves do not propagate over long distances [7].

Underwater acoustic propagation is a technique that has been widely used in communications over the past two decades, due the great distances sound travels in this environment. However, the acoustic wave offers limited bandwidth since the characteristics vary with time and are dependent on the location of the transmitters [8]. Besides, temperature, salinity, ambient noise, turbidity affect acoustic propagation, leading to attenuation, delay spreading and the interference patterns caused by multipath effects.

Existing techniques for underwater acoustic transmissions are at this time mature enough to face the challenges of high data rate needed for real-time transmission [9]. However, in order to have a successful transmission, mainly for high image and video data rates, the understanding of the communication channel is extremely important.

Because data transmission rates are environment dependent, the techniques for data processing or compression may not be enough whether the underwater medium is not previously analyzed. The acoustic channel simulation includes the effects of attenuation over the channel, and addition of noise from the recordings [9]. Thus, this step for applying acoustic propagation modeling techniques is one of the first studies required for the system implementation.

The main goal of the present work is to point some aspects of the acoustic channel, showing its complexity due the oceanographic parameters that influence the acoustic propagation. A ray-tracing acoustic model is used to simulate transmission loss of modem signals in this complex and dynamic medium. As the environmental conditions evolve in time, the model analysis can be repeated in order to predict on how the acoustic transmission may behave, so as to map the best modem choice and position to establish the channel communication.

This research is motivated by the necessity of developing efficient monitoring systems for underwater applications. Finally, a comparative study of the performance between three types of acoustic telemetry modems based on predictions of the propagation acoustic model is presented.

2. CASE STUDY: CAMPOS BASIN

The Campos Basin is the main sedimentary area already explored on the Brazilian coast. With an area of approximately 100,000 km², 48 production platforms operated by Petróleo Brasileiro S.A. (Petrobras) and an exploration volume of

1,734,705 barrels per day, it is the largest oil province in Brazil, responsible for more than 80% of the national oil production. Besides, it has the largest reserves already identified and classified in the country, being a reference for exploration and production in deep and ultra-deep waters [10-11]

The basin extends from Cabo Frio, Rio de Janeiro State (42°W 23°S) to the mediations of Vitória, Espírito Santo State (40°24'W 20°30'S). The waters present on the slope and in the oceanic area of the Campos basin are characterized mainly by the horizontal and vertical distribution of four types of water masses: Tropical Water (TW), South Atlantic Central Water (SACW), Antarctic Intermediate Water (AIW) and North Atlantic Deep Water (NADW). Winds from the northeast quadrant and its components influence the area throughout the year. During the autumn season such propensity continues to be noticed, but to a lesser extent, because the South Atlantic Subtropical Anticiclone (SASA) is further away from the coast, reducing its influence [12].

The Atlantic Oceanographic & Meteorological Laboratory of the National Oceanic & Atmospheric Administration (NOAA) gathers data from oceanographic cruises conducted in the Atlantic Ocean, where XBTs were launched to collect these data [13]. The data between 1994 and 2016 are available on the website. The stations chosen for the simulation are illustrated in Figure 1:

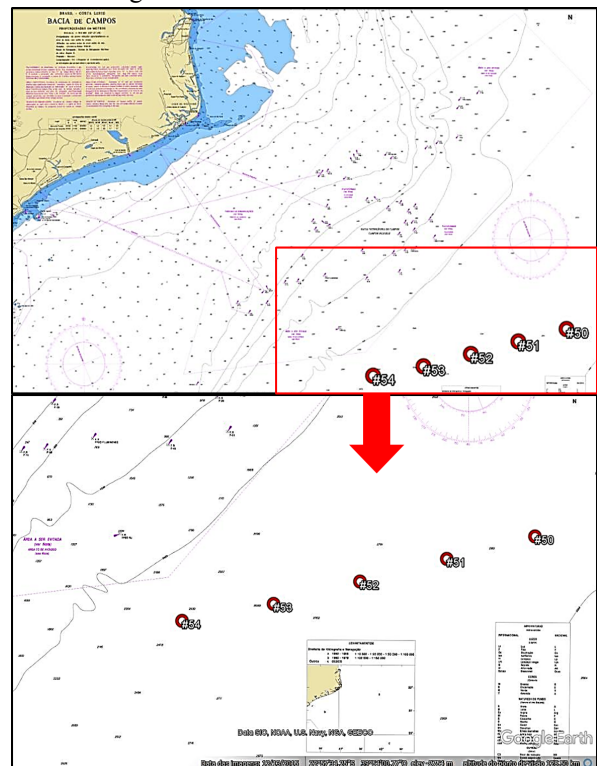


Figure 1: Campos Basin data acquisition stations.

Five profiles of the transect were chosen of the AX97 cruise, performed in April 2016. These profiles correspond to the stations 50, 51, 52, 53 and 54 of the cruise. The position of the stations is listed in the Table I:

Table I: Position of the stations for case study

Station	Latitude	Longitude
#50	22°51'25.20"S	39°19'58.80"W
#51	22°54'28.80"S	39°33'3.60"W
#52	22°57'32.40"S	39°45'54.00"W
#53	23° 0'32.40"S	39°58'40.80"W
#54	23° 2'49.20"S	40°12'14.40"W

The sediment of the basin is mainly composed of fine sand and mud, which corresponds to a sediment sound speed, density and attenuation of approximately 1635 m/s, 1.75 g/cm³ and 0.65 dB/m, respectively [14-15].

The data used in the present work were collected during autumn, where the weakening of the north-easterly winds was observed, predominating southwest winds, with mean wind speed around 16 knots (8.23 m/s) and south winds, with mean wind speed around 8 knots (4.11 m/s) [12]. The temperature along the stations showed an average of 27.3°C in the surface and 5.5°C at the maximum depth measured. The salinity presented an average over the seasons of 36.8 psu in the surface and 34.4 psu at the maximum depth measured.

The Sound Speed Profile (SSP) was obtained from Chen and Millero's equation by using data acquired by XBT measurements. These profiles include pressure, salinity, temperature and depth data [16]. As the sound speed profile and temperature profile variation between the stations present a small difference between the collected samples, a unique profile was used for each one. The SSP of the transect (Figure 3) was used as an input in the model, since it represents the average of sound speed data from all stations.

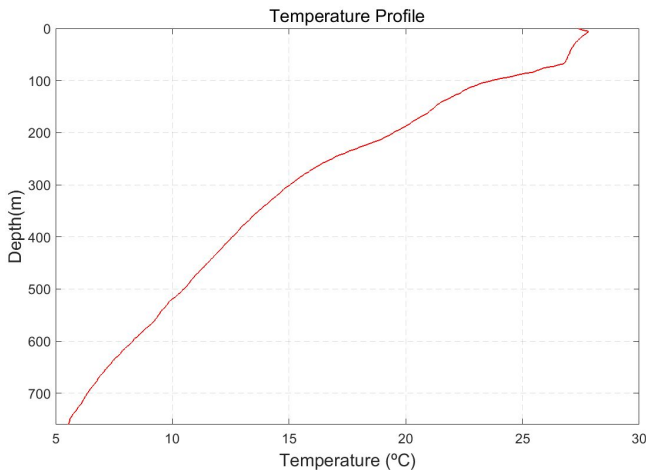


Figure 2: Temperature profile for the transect.

Figure 2 represents the temperature profile for the same depth range. Note that the temperature decreases with the increasing depth. It is also possible to see the mixed layer in the first 100 m and the thermocline below the superficial layers.

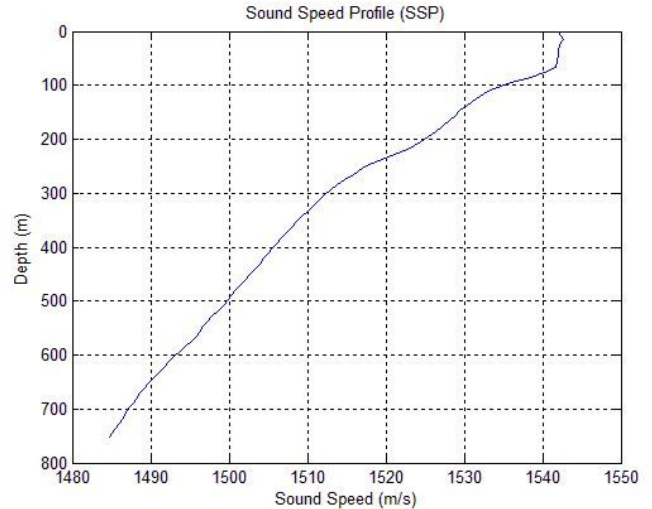


Figure 3: Sound Speed Profile (SSP) for the transect.

The SSP graph is presented in Figure 3, where the maximum depth is 760 m, corresponding to the deepest range obtained from XBT measurements during the NOAA experiment. The deep layer, where the temperature decreases in a more slowly way, is not shown in the plot. The sound speed on the surface was approximately 1540 m/s while in the deepest layers it reached a minimum value of 1485 m/s.

3. MODELING OF THE ACOUSTIC PROPAGATION CHANNEL

When compared to terrestrial wireless communication channel, the modeling of the submarine wireless channel is quite complex and dependent on the limiting conditions of the medium [17]. Intrinsic phenomena, caused by the propagation environment dynamics makes it a great challenge to implement wireless communication channel in these environments.

When an acoustic signal is transmitted from the source to the receiver, part of the energy is lost in the medium and the capacity of the systems depends on the conditions and the characteristics of the propagation channel. In order to estimate the detection capacity of the signals according to the medium characteristics, this section presents the characterization of the parameters that influence the acoustic propagation channel.

2.1 Transmission Loss

Transmission Loss (TL) is a combination of both spreading loss and absorption loss. Spreading loss is a geometrical effect representing the regular weakening of a sound signal as it spreads outward from the source [18]. The absorption coefficient can be obtained empirically by using Thorp's approximation [19]. The absorption loss represents a true acoustic energy loss to the medium where the propagation occurs [20]. The following equation is generally valid for frequencies above a few hundred Hz, considering $a(f)$ the absorption coefficient in dB/km and frequency f in kHz [21]:

$$10 \log a(f) = 0.11 \frac{f^2}{1+f^2} + 44 \frac{f^2}{4100+f^2} + 2.75 \cdot 10^{-4} f^2 + 0.003 \quad (1)$$

Figure 4 represents the estimation for the absorption coefficient in dB/km for frequencies from 0 to 100 kHz. According to the figure, it is possible to observe the absorption coefficient increasing with the increase of the frequency.

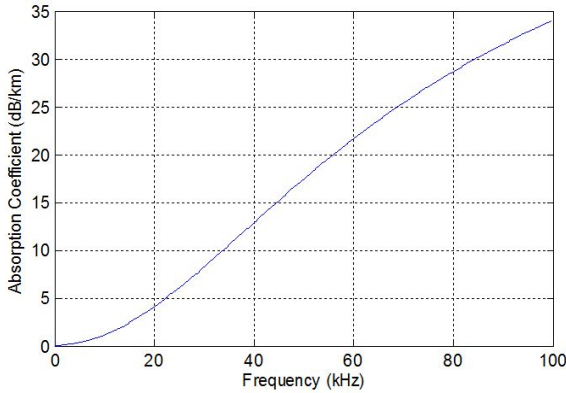


Figure 4: Absorption coefficient for frequencies from 0 to 100 kHz.

The path loss will be the result of both spreading loss and absorption loss and can be expressed as follows [22]:

$$10 \log A(l, f) = k \cdot 10 \log l + l \cdot 10 \log a(f) \quad (2)$$

The spreading factor $k = 1$ represents a cylindrical spreading, while $k = 2$ is spherical and $k = 1.5$ represents the practical spreading [18] and l is the range in km.

The path direct model considers the underwater environment as a homogeneous unbounded medium, so transmission loss (TL) is caused due the spherical spreading and absorption can be expressed as follows [18]:

$$TL = 20 \log l + a(f) l \times 10^{-3} \quad (3)$$

where, $a(f)$ is the absorption coefficient expressed in dB/km and l is the transmission range in meters.

2.2 Level Noise

The underwater environment is highly noisy. Though noise characterization is an important task, since the noise presence may limit the performance of communication systems, this is not a trivial task. The noise in submarine acoustic channel depends at the same time on the ambient noise and on the noise produced in specific areas. Some types of noises found in the ocean are: Turbulence (N_{tb}), Shipping (N_{sh}), Waves (N_{wv}) and Thermal Noise (N_{th}) [23]. The modeling of the Noise Level (NL) in the ocean can be obtained from the Power Spectral Density (PSD) of energy (dB re μPa) of each source of noise as a function of frequency (kHz) as shown in the empirical formula [22]:

$$10 \log N_{tb}(f) = 17 - 30 \log f, \quad (4)$$

$$10 \log N_{sh}(f) = 40 + 20(s - 5) + 26 \log f - 60 \log(f + 0.03), \quad (5)$$

$$10 \log N_{wv}(f) = 50 + 7.5w^{1/2} + 20 \log f - 40 \log(f + 0.4), \quad (6)$$

$$10 \log N_{th}(f) = -15 + 20 \log f, \quad (7)$$

where f is the frequency, s and w are the shipping and wind variables, respectively. The total power spectral density of the ambient noise at different frequencies is given by empirical formula.

$$NL(f) = N_{tb}(f) + N_{sh}(f) + N_{wv}(f) + N_{th}(f) \quad (8)$$

Figure 5 depicts the noise power spectrum level in dB re μPa based on the empirical formula. The ship factor ($s=0$) was considered as light, and in this area wind speed is around 8.23 m/s (16 knots).

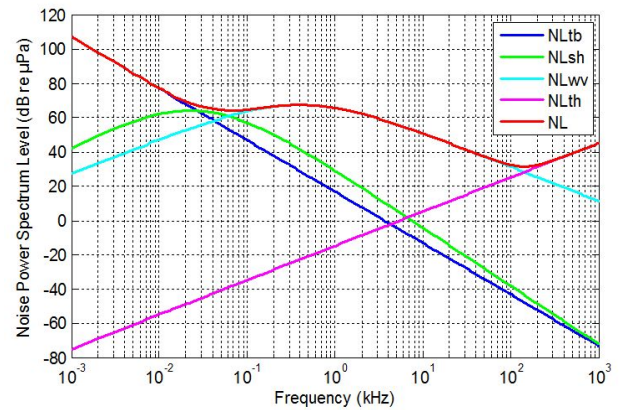


Figure 5: Ambient Noise Level (Power Spectral Density) for $s=0$ and $w= 8.23$ m/s.

For frequencies above 100 kHz it is possible to verify the predominance of thermal noise. Between 10 Hz and 100 Hz, the shipping noise shows a higher value if compared to other

frequency bands. The contribution of wave driven noise is predominant from 100 Hz to 100 kHz, when it begins to decrease. For frequencies below 10 Hz, turbulent noise has the major contribution.

The choice of the operating frequency of the acoustic modems is directly related to the physical parameters mentioned in this section.

4. ACOUSTIC CHANNEL MODELING

The simulations presented in this work were done through a implementation of the ray tracing model BELLHOP in MATLAB, which predicts acoustic pressure fields in ocean environment. Despite of authors implementation, it is also included in the MATLAB *Acoustics Toolbox* (available on *Ocean Acoustics Library* website) [24-25]. The method computes acoustic fields via Gaussian beam tracing and it can include range-dependent bathymetry [26-27].

The computational simulation run in this article was implemented through an algorithm developed in the MATLAB software program. The equations are used to calculate the coordinates, phase, amplitude and delay [24].

BELLHOP model was chosen because of its capability of dealing with deep water environments. Besides, it can handle high frequency simulations. This turns the BELLHOP model physically and computationally applicable to predict transmission loss in this case. The input data for the simulations are environmental parameters, such as sound speed profile of the medium, bathymetry and geoacoustic properties of the bottom.

In this work, the parameters of three modem models with different frequencies were selected as shown in Table II. The transmission loss was calculated through BELLHOP model according to the operating frequency of each equipment and considering the source positioned at a depth around 744 m and the receiver away at a maximum horizontal distance of 5 km.

Table II: Parameters of Underwater Acoustic Modems

Modem	Frequency (kHz)	Bandwidth (kHz)	Data Rate (bps)	Power Consumption (W)	Max Distance (m)
A	9.75	4.5	2000	20	5000
B	35695	17.85	17800	1	1000
C	48 - 78	30	31200	18	1000

As discussed in the previous sections, the increase in frequency leads to the attenuation increase and as a consequence, limitations on the transmission range. On the other hand, although lower frequencies guarantee lower rates of useful data for signal transmission, limits the application of these equipment for the signal transmission at high data rates, necessary in the case of the images transmission.

Underwater image communication in a higher transmission speed and a lower Bit Error Rate (BER) is a challenge due the complexity of the underwater acoustic channel. Some authors suggest systems for real-time underwater image communication capable of resisting multi-path interference, reducing BER and increasing communication rate [28].

Therefore it is necessary to find a tradeoff regarding the choice of the modem. Through modeling, it is possible to predict the effect of signal propagation and to estimate the performance of the modems considering the simulated environment conditions. Figures 6, 7 and 8 show model results, where TL values are shown for different acoustic modem models.

Figure 6 shows the TL results for 9.75 kHz, which is the frequency operation of the modem A. According to the graphic, the TL reaches 75 dB approximately at the maximum operation distance, i.e, at 5 km. For distances under 1 km, the plot shows a lower transmission loss, reaching 60 dB approximately.

The results show that the TL presents a great variation along the water column due the destructive or constructive interference patterns caused by the multipath effects.

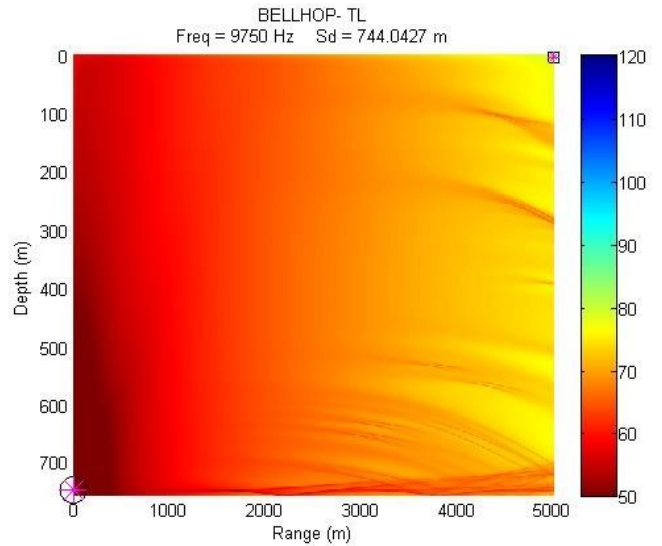


Figure 6: Transmission loss (TL) in dB as a function of range and depth for a 9.75 kHz source at water depth of 744 m.

The results presented in Figure 7 were calculated for 35.69 kHz, which is the frequency operation of modem B. The plot shows that from a distance of 5 km, the signal was drastically attenuated. At this distance, the transmission loss increases to 120 dB.

As expected, the model output shows that although the modem B offers higher transmission rates, the high operating frequency limits its transmission range. At the maximum

operating distance, i.e, at 1 km the transmission loss is approximately 70 dB.

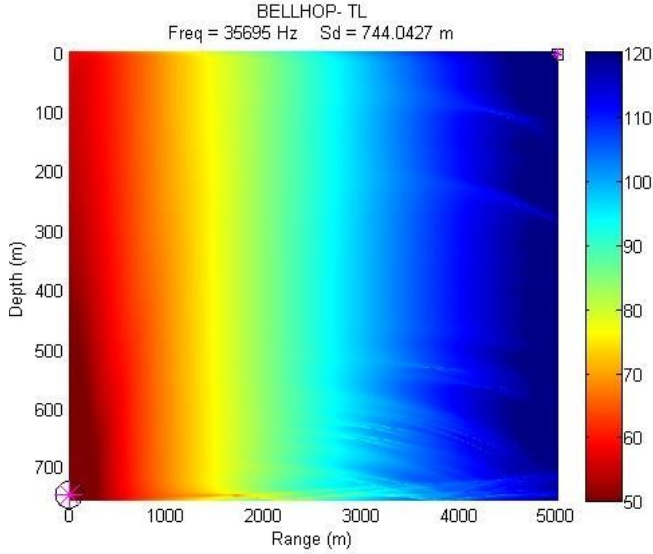


Figure 7: Transmission loss (TL) in dB as a function of range and depth for a 35.69 kHz source at water depth of 744 m.

For even higher frequencies, as for modem C where the maximum frequency is 78 kHz, the transmission loss of 85 dB approximately it is reached at 1 km distance, as can be seen at Figure 8.

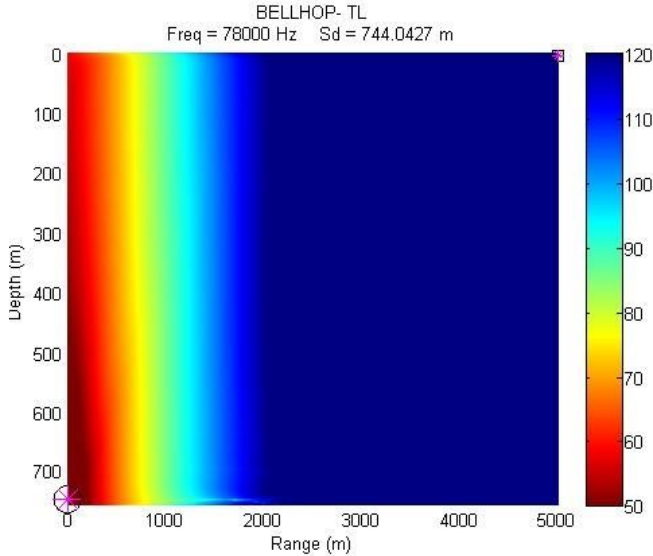


Figure 8: Transmission loss (TL) in dB as a function of range and depth for a 78 kHz source at water depth of 744 m.

5. UNDERWATER ACOUSTIC MODEMS SIGNAL TO NOISE RATIO (SNR)

In order to obtain the Signal to Noise Ratio (SNR) in an acoustic channel, it is necessary to consider both the Transmission Loss ($TL(d, f)$) and the total noise power spectral density ($NL(f)$) of acoustic signal. When the transmitted signal has a frequency of f and power (P), the SNR is given by [22]:

$$SNR(d, f) = \frac{P/TL(d, f)}{N(f) \Delta f} \quad (9)$$

where Δf is the received noise bandwidth (a narrow band around the frequency f). The $TL(d, f) \times N(f)$ product gives the frequency-dependent part of SNR and the factor $\frac{1}{TL(d, f)N(f)}$ defines the effect of transmission loss and noise in dB for different transmission distances and frequency values [21-22]

The results obtained using the frequencies of the A, B and C modems and the equations presented in this article for absorption ($a(f)$), transmission loss (TL), noise level $NL(f)$ and SNR are presented on Table III. The $a(f)$ and $NL(f)$ values have been withdrawn from plots 4 and 5, respectively.

Table III: Results of the Physical Medium of the Channel

Modem	Freq. (kHz)	$a(f)$ dB/km	TL (dB) from Bellhop	TL (dB) from Eq 3	NL dB re μ Pa	SL (dB)	SNR (dB) from TL Bellhop	SNR (dB) from TL Eq.3
A	9.75	1.13	60	61.13	51.04	153.75	42.71	41.58
B	35.69	10.89	70	70.89	40.29	140.74	30.45	29.56
C	78	28.07	85	88.08	33.94	153.29	34.35	31.27

From Table III, it is possible to notice that for modem A, whose operating frequency is low, the main responsible for the signal attenuation is the noise while for modem C, whose frequency is eight times greater, the main responsible for the attenuation is the absorption.

The TL values were obtained using Equation 03 and from the results obtained through computational modeling. The values show an increase in transmission loss obtained with the results of the Bellhop model in relation to the value calculated by the equation. The results are consistent since the transmission loss obtained from the model takes into account the multipath propagation resulting from the ray interactions at the boundaries (bottom and surface).

The SNR value was calculated using the passive sonar equation [20]:

$$SNR = SL - TL - NL + DI \quad (10)$$

where,

SL = Source Level (dB);

TL = Transmission Loss (dB);

NL = Noise Level, dB;

DI = Directivity Index, in dB;

The DI was adjusted to 0 dB considering an omnidirectional field of transducer radiation and the source level (dB) was calculated using Equation 11 [18]:

$$SL = 10 \log \frac{I_t}{0.67 \times 10^{-18}} \quad (11)$$

where, I_t is the intensity in $Watt/m^2$. The transmission power was extracted from Table II that specifies the power consumption of the modem used.

According to Table III, considering the operation distance under 1 km and comparing the performance of the modems, the SNR results show a higher SNR for modem A, i.e. in the operation frequency of 9.75 kHz the system achieves the maximum SNR of 42.71 dB. However in this frequency, the data rates are much lower, of only 2000 bps, that unfeasible the communication system application for images transmission.

It is important to note that the power efficiency is also an important requirement for underwater data transmission systems and although the SNR value for modem C (34.35 dB) is higher than SNR for modem B (30.45 dB), according to Table II, the power consumption of modem B is of 1 W, much lower than the power for modem C that is 18 W.

Thus, to achieve the requirements for the deployment of an underwater communication system, it is necessary to take into account at the same time the limitations of the propagation channel as well as the parameters of the transmission equipment.

6. CONCLUSIONS

In this paper, we assess the feasibility of using the underwater acoustic channel for data transmission in subsea environments. The understanding of the characteristics of the Campos Basin environment was essential, since they influence the acoustic channel and consequently, the performance of the telemetry modems. The parameters of three modem models with different operation frequencies were selected and analyzed in order to obtain the Signal to Noise Ratio (SNR) of the transmission signal. The acoustic modem choice is directly related to the physical parameters determined in this work.

Given the system characteristics (frequency, data rate, bandwidth, power consumption and distance) inside the environment, one can decide on which system is more

appropriate or viable, by quantifying its limitations in terms of signal-to-noise ratio and range, evaluating in this manner the communication channel.

Because of the availability of expressions to calculate the SNR, the methodology used has a wide range of applicability for evaluating different underwater acoustic modems. The BELLHOP model for transmission loss estimation allows the analysis of a large number of scenarios including deep water environments.

The signal-to-noise ratio is a key factor in a communication system and the challenges currently lie in reaching both optimal signal-to-noise ratio and high data rate. Potential works for the future are to perform in situ tests for validation of the results and further evaluations on the operation in dynamic environments, networking capability, interoperability and real time data acquisition.

ACKNOWLEDGMENTS

The authors acknowledge the Oceanographic and Atmospheric Meteorological Laboratory of the National Oceanic and Atmospheric Administration (NOAA) for the availability of XBT data obtained from oceanographic cruises.

REFERENCES

- [1] Aminzadeh, F. and Purohit, A. D., 2013, "Optimal Wireless Sensor Networks for Reliable Low Cost Smart Oilfields," *SPE Digit. Energy Conf.*, no. March, pp. 5–7.
- [2] Hongtao, Z., Shengjun, X., Zhijie, Y. U. E. and Zhongkang, W., 2016, "Sea Trials of an Underwater Acoustic Network in the East China Sea 2015", *2016 IEEE/OES China Ocean Acoustics (COA) Symposium*, Harbin, pp. 1-5.
- [3] Du, X. and Liu, X., 2016, "Underwater Acoustic Networks Testbed for Ecological Monitoring of Qinghai Lake," *OCEANS 2016 - Shanghai*, Shanghai, pp. 0–3.
- [4] Wu, C., Kung, H., Kuo, L., Chen, C. and Tasi, K., 2007, "Disaster Prevention Information System Based on Wireless / Mobile Communication Networks", *The Seventeenth International Offshore and Polar Engineering Conference*, Lisbon, pp. 1863–18707.
- [5] Liu, L., Zhou, S. and Cui, J., 2008, "Prospects and Problems of Wireless Communication for Underwater Sensor Networks", *Wireless Communications and Mobile Computing*, vol. 8, pp. 977–994.
- [6] Che, X., Wells, I., Dickers, G., Kear, P. and Gong, X., 2010, "Re-evaluation of RF electromagnetic communication in underwater sensor networks," *IEEE Communications Magazine*, vol. 48, no. 12, pp. 143–151.

- [7] Ahmed, R. and Stojanovic, M., 2016, “Joint Power and Rate Control for Packet Coding over Fading Channels,” *IEEE Journal of Oceanic Engineering*, vol. PP, no. 99, pp. 1-14.
- [8] Stojanovic, M., 2003, “Underwater acoustic communications”, *IEEE Communications Magazine*, vol. 47, no. 1, pp. 435–440.
- [9] Ribas, J., Sura, D., and Stojanovic, M., 2010. “Underwater Wireless Video Transmission for Supervisory Control and Inspection using Acoustic OFDM”, *OCEANS 2010 MTS/IEEE SEATTLE*, Seattle, WA, pp. 1-9.
- [10] Agência Natural do Petróleo, Gás Natural e Biocombustíveis (ANP), 2017, “Boletim de Produção de Petróleo e Gás Natural”, from <http://www.anp.gov.br/?pg=73557&m=&m=&t1=&t2=&t3=&t4=&ar=&ps=&cachebust=1421426738803>
- [11] Petrobras, 2017, “Bacia de Campos”, from <http://www.petrobras.com.br/pt/nossas-atividades/principais-operacoes/bacias/bacia-de-campos.htm>
- [12] Dereczynski C. and Menezes, W., 2015. “Meteorologia da Bacia de Campos”, *Caracterização Ambiental Regional da Bacia de Campos, Atlântico Sudoeste*, 1st edition, Elsevier, Rio de Janeiro.
- [13] National Oceanic and Atmospheric Administration (NOAA), 2016. “High Density XBT Transects”, from <http://www.aoml.noaa.gov/phod/hdenxbt/index.php>
- [14] Figueiredo Jr., A. G. and Pacheco, C. E. P., 2015, “Sedimentologia e Geomorfologia da Bacia de Campos, Brasil”. *Geologia e Geomorfologia*, Elsevier, Rio de Janeiro, vol. 1. p. 13-32.
- [15] Hamilton, E. L., 1980, “Geoacoustic modeling of the sea floor”, *The Journal of the Acoustical Society of America*, vol. 68, n.5, pp 1313-1340.
- [16] Chen, C. T. and Millero, F. J., 1977, “Speed of sound in seawater at high pressures”, *The Journal of the Acoustical Society of America*, vol. 62, n.5, pp 1129-1135.
- [17] Chaitanya, D., Sridevi, C., Rao, G., 2011, “Path loss analysis of Underwater communication systems”, *Students’ Technology Symposium (TechSym), 2011 IEEE*, Kharagpur, pp. 65–70.
- [18] Anandalatchoumy, S. and Sivaradje, G., 2015, “Comprehensive Study of Acoustic Channel Models for Underwater Wireless Communication Networks”, *International Journal on Cybernetics & Informatics*, vol. 4, no. 2, pp. 227–240.
- [19] Harris, A. F. and Zorzi, M., 2007, “Modeling the underwater acoustic channel in ns2”, *Proceedings of the 2nd International Conference on Performance Evaluation Methodologies and Tools ICST*, Nantes, France, pp. 1–8.
- [20] Urlick, R., 1983, “Principles of Underwater Sound”, 3rd edition, McGraw-Hill, New York.
- [21] Berkhovskikh, L. and Lysanov, Y., 1982, “Fundamentals of Ocean Acoustics”, 1st edition, Springer-Verlag, Berlin Heidelberg.
- [22] Stojanovic, M., 2007, “On the relationship between capacity and distance in an underwater acoustic communication channel”, *ACM SIGMOBILE Mobile Computing and Communications Review*, vol. 11, no. 4, p. 34.
- [23] Melodia, T., Kulhandjian, H., Kuo, L. and Demirors, E., 2013, “Advances in Underwater Acoustic Networking”, *Mobile Ad Hoc Networking: Cutting Edge Directions*, Second Edition, John Wiley & Sons, Inc., Hoboken, pp. 804–854.
- [24] Porter, M. B., 2011, “The BELLHOP Manual and User's Guide: Preliminary Draft”, Heat, Light, and Sound Research, Inc., La Jolla, CA, USA, Tech. Rep.
- [25] U.S. Office of Naval Research, 2016, “Ocean Acoustics Library”, from <http://oalib.hlsresearch.com>
- [26] Porter, M. B., 1991, “The KRAKEN normal mode program”, SACLANT Undersea Research Centre Memo, SM-245.
- [27] Porter, M. B. and Bucker, H. P., 1987, “Gaussian beam tracing for computing ocean acoustic fields”, *The Journal Acoustical Society of America*, vol. 82, 1349–59.
- [28] Yina, Lu., Chen, B., Hu, J., and Cai, P., 2011, "Research on the Key Technologies for Underwater Image Communication System", *Procedia Engineering*, vol. 24, pp 610-615.